



Estimation of Reference Crop Evapotranspiration Using Backpropagation Neural Network Model

역전파 신경망 모델을 이용한 기준 작물 증발산량 산정

Minyoung Kim^a · Yonghun Choi^{b,†} · Susan O'Shaughnessy^c · Paul Colaizzi^d ·
Youngjin Kim^e · Jonggil Jeon^f · Sangbong Lee^g

김민영 · 최용훈 · 수잔 오샤네시 · 폴 콜레이지 · 김영진 · 전종길 · 이상봉

ABSTRACT

Evapotranspiration (ET) of vegetation is one of the major components of the hydrologic cycle, and its accurate estimation is important for hydrologic water balance, irrigation management, crop yield simulation, and water resources planning and management. For agricultural crops, ET is often calculated in terms of a short or tall crop reference, such as well-watered, clipped grass (reference crop evapotranspiration, ET₀). The Penman-Monteith equation recommended by FAO (FAO 56-PM) has been accepted by researchers and practitioners, as the sole ET₀ method. However, its accuracy is contingent on high quality measurements of four meteorological variables, and its use has been limited by incomplete and/or inaccurate input data. Therefore, this study evaluated the applicability of Backpropagation Neural Network (BPNN) model for estimating ET₀ from less meteorological data than required by the FAO 56-PM. A total of six meteorological inputs, minimum temperature, average temperature, maximum temperature, relative humidity, wind speed and solar radiation, were divided into a series of input groups (a combination of one, two, three, four, five and six variables) and each combination of different meteorological dataset was evaluated for its level of accuracy in estimating ET₀. The overall findings of this study indicated that ET₀ could be reasonably estimated using less than all six meteorological data using BPNN. In addition, it was shown that the proper choice of neural network architecture could not only minimize the computational error, but also maximize the relationship between dependent and independent variables. The findings of this study would be of use in instances where data availability and/or accuracy are limited.

Keywords: Reference crop evapotranspiration; Penman-Monteith equation (FAO 56-PM); Backpropagation neural network (BPNN) model; meteorological variables

초 록

작물 증발산량은 수자원 계획 및 관리, 물수지 분석, 작물 관개 계획 및 생산량 추정 등에 널리 활용되고 있으며, 특히 FAO에서 공인한 Penman-Monteith식 (FAO 56-PM)은 잠재 증발산량 산정을 위한 표준방법으로 많이 사용되고 있다. Penman-Monteith식을 이용한 잠재증발산량 산정은 최소온도, 평균온도, 최대온도, 상대습도, 풍속과 일사량인 6가지 항목에 대한 시계열 자료가 필요한데, 결측 또는 미계측된 경우에는 사용이 어려운 단점을 가지고 있다. 따라서, 본 연구에서는 역전파 신경망(BPNN) 모델을 이용해서 6개 미만의 기상항목으로도 잠재증발산량이 추정가능한지를 확인하였다. 여섯 가지 기상항목을 각각 1~6개의 조합으로 입력자료를 구성하고, BPNN 모델을 이용해서 학습, 검증 및 테스트를 한 결과, 입력 자료가 많아질수록 좋은 결과가 산출되었으며, 일사량, 최대온도와 상대습도만으로 결정계수(R²)가 0.94정도로 비교적 높은 예측결과를 얻을 수 있었다. 또한 산정 오차를 줄이고, 항목간의 상관관계를 높이기 위해서는 역전파 신경망 구조의 적절한 선택이 중요한 것으로 확인되었다. 역전파 신경망 모델을 사용하면 요구되는 기상 항목과 데이터의 양에 대한 제약 없이 예측이 가능할 수 있기 때문에 기준 증발산량 산정에 유용하게 활용될 수 있을 것이며 향후 작물 재배를 위한 적정 관개계획 수립에도 유용하게 사용될 것이라 사료된다.

주제어: 기준 작물 증발산량; Penman-Monteith식(FAO 56-PM); 역전파 신경망 모델; 기상변수

^{a, c, f, g} Agricultural Researcher, Department of Agricultural Engineering, National Institute of Agricultural Sciences (NAS), Rural Development Administration (RDA)

^b Post-doctoral researcher, Department of Agricultural Engineering, National Institute of Agricultural Sciences (NAS), Rural Development Administration (RDA)

^{c, d} Agricultural Engineer, Conservation and Production Research Laboratory, United States Department of Agriculture, Agricultural Research Service (USDA-ARS)

† **Corresponding author**

Tel.: +82-63-238-4161 Fax: +82-63-238-4145

E-mail: yhchoi82@korea.kr

Received: October 1, 2019

Revised: November 7, 2019

Accepted: November 8, 2019

I. INTRODUCTION

Evapotranspiration is one of the hydrologic cycle components and combines two distinct processes which are the evaporation of water directly from the ground surface and transpiration through the plants' stomata (Allen et al., 2006). Knowledge of the reference crop evapotranspiration (ET_0) is very important in various fields of water resources such as estimation of crop water requirements, scheduling of irrigation water application, modeling of rainfall-runoff process and evaluation of land suitability (Djaman, et al., 2018). Because of its significance, various indirect and direct methods have been used to determine ET_0 .

Direct methods include field measurements using lysimeters and pan evaporimeters to quantify evapotranspiration (Parisi et al., 2009; Lu et al., 2018), however, these methods are time-consuming. Furthermore, time, labor and high skill for data collection and communication are required to improve estimates and spatial interpolation, which may be inappropriate for large-scale studies (Palayaso, 1965). On the other hand, methods using micro-meteorological measurements such as the energy balance Bowen ratio and eddy covariance flux measurement systems have also been employed to measure surface heat fluxes but these are expensive and complex, both of which limit their wide applicability (Drexler et al., 2004).

Due to limitations associated with direct methods, the adoption of indirect methods of physical mathematical formulations has become a preferred and practical alternative to ET_0 estimation (Allen et al., 2011). ET_0 is a complex process which is dependent on several interacting climatological factors, such as temperature, humidity, wind speed and radiation. The lack of physical understanding of the ET_0 process and the unavailability of all relevant data results in inaccurate estimation of ET_0 (Vyas and Subbaiah, 2016). Consequently, significant research activities have been carried out to develop and/or implement reliable and accurate prediction models that use observed weather data (air temperature, relative humidity, solar radiation and wind speed) as inputs to estimate ET_0 (Jensen et al., 1990; Allen et al., 1998; Jennifer and Sudheer, 2001; George et al., 2002; Itenfisu et al., 2003).

The Penman-Monteith equation (FAO 56-PM) is maintained as the single standard method recommended by the FAO for the computation of ET_0 from complete meteorological data (Smith et al., 1992; Allen et al., 2006). Several models such

as Hargreaves & Blaney-Criddle and other models have been proposed to predict ET_0 , but Traoré et al. (2008) reported that these models do not have universal consensus for different climatic conditions. Even though its modeling accuracy is well known, the main shortcoming of the FAO 56-PM method is its requirement of a large number of meteorological data that are not always available in many locations. For this reason, numerous attempts have been tried to overcome difficulties associated with data availability for ET estimation (Dai et al., 2009).

To address this, past studies investigated the application of Artificial Neural Networks (ANNs) and assessed their performance with limited number of datasets rather than a full set of data (minimum, average & maximum air temperature, relative humidity, wind speed and solar radiation). ANNs have been intensively used in modeling complex nonlinear processes (e.g., rainfall-runoff, stream flow, ground water, precipitation and evapotranspiration) because they have the ability to map the input-output relationships without a complete understanding of the physical processes (Choi et al., 2018). Lee et al. (2010) showed the good performance of ANNs in estimating future reference crop evapotranspiration. Abedi-Koupai et al. (2009) evaluated the performance of ANNs with the conventional methods (Penman, Penman-Monteith, Stanghellini and Fynn) to estimate reference evapotranspiration and they found that the efficiency value of ANNs was superior than others. Sudheer and Jain (2003) and Zanetti et al. (2007) in their ET estimation simplified the neural network inputs to air temperature, extraterrestrial solar radiation and daily light hours. Khoob (2008) used similar input sets but without the daily light data for successfully estimating ET in Iran.

The objectives of this study were to adopt a Backpropagation neural network (BPNN) model to calculate daily ET_0 from different input combinations (minimum, average & maximum air temperature, relative humidity, wind speed and solar radiation) and to assess the computational performance of ET_0 values between BPNN and Multiple Linear Regression (MLR).

II. MATERIALS AND METHODS

1. Description of Study area and Meteorological data

A total of six meteorological variables were collected from a weather station which was located at the experimental station

in USDA Agricultural Research Service Conservation and Production Research Laboratory, Bushland, Texas, USA (35° 11' N, 102° 6' W, 1,170 m above MSL) (Fig. 1). Data from periods (May – December, 2010, January – December, 2012 and January, 2014 – October, 2017) were used and any faulty data due to sensor malfunction were deleted. All required data, average, minimum and maximum air temperature (T_{avg} , T_{min} and T_{max} , °C), relative humidity (RH, %), wind speed (WS, m/s) and solar radiation (SR, watt/m²), were measured at 6 second intervals, reported as 15 minutes mean values from a weather station, and then stored in a Datalogger (Campbell Scientific, CR3000, Logan, Utah, USA). Sensors used were temperature & relative humidity sensor (HC2S3, Rotronic, Hauppauge, New York, USA), pyranometer (LI200-RX, LI-COR, Lincoln, Nebraska, USA), and wind sentry set (Model 03002-L, R.M. Young, Traverse City, Michigan, USA).



Fig. 1 Description of study area

2. Computation of reference crop evapotranspiration using the FAO 56-PM equation

The FAO 56-PM equation was developed to quantify the amount of water loss from soil surface and plant leaf through evaporation and transpiration. This equation accounts for aerodynamic as well as physiological parameters and requires large data inputs (T_{min} , T_{avg} , T_{max} , WS, RH and SR). The equation is as follows (Allen et al., 1998):

$$ET_0 = \frac{0.408\Delta(R_n - G) + \gamma \frac{900}{T + 273} u_2 (e_s - e_a)}{\Delta + \gamma(1 + 0.34u_2)} \quad (1)$$

where ET_0 is reference crop evapotranspiration [mm day⁻¹], R_n is net radiation at the crop surface [MJ m⁻² day⁻¹], G is soil heat flux density [MJ m⁻² day⁻¹], T is average daily air temperature at 2 m height [°C], u_2 is wind speed at 2 m height

[m s⁻¹], e_s is saturation vapor pressure [kPa], e_a is actual vapor pressure [kPa], $(e_s - e_a)$ is saturation vapor pressure deficit [kPa], Δ is slope vapor pressure curve [kPa °C⁻¹], and γ is Psychrometric constant [kPa °C⁻¹].

The FAO 56-PM equation requires daily data as inputs, therefore, all necessary data collected from a weather station were converted from every 15 minutes to daily averages (T_{min} , T_{avg} , T_{max} , RH and WS) and sums (SR) to apply to the FAO 56-PM equation.

3. Application of BPNN and MLR models

The Multi-Layer Perceptron (MLP), a traditional Artificial Neural Network, is known as the common, effective and successful neural network architecture which uses a supervised learning and technique called Backpropagation (BP) algorithm. Backpropagation neural network (BPNN) is by far the most popular (Haykin, 1998), performs parallel training for improving the efficiency of MLP networks, and derives the network error which is fed back into the network model and used to adjust the weights (Kecman, 2001; Mia et al., 2015). The MLP consists of at least three layers, an input layer, one or more hidden layer, and an output layer. Adjustable weights are used to connect the nodes between adjacent layers and optimized by the training algorithm to obtain the desired results. Through that process, the error in prediction decreases with each iteration, succeeds when the neural network model reaches the specified level of accuracy and produces the desired outputs (Kim et al., 2008). First of all, this study begun with three layer learning network which consists of an input layer, a hidden layer and an output layer (Fig. 2), but during the training procedure, more than one hidden layers were evaluated to calculate the weighted inputs with activation functions to produce the better outputs. In designing a robust and accurate ANN model, the modeler must address a number of important factors, including the type and structure of the neural network, the input prediction variables used, and data pre-processing. This was generally accomplished through a combination of best professional judgment, heuristic rules, and trial & error (Laaboudi et al., 2012). The governing factors in BPNN includes: a number of hidden layers, a number of hidden processing elements (PEs), the transfer function (e.g., sigmoid, tan-sigmoid), learning algorithm (e.g., Delta, extended DBD) and learning parameters (e.g., learning rate, momentum factor, initial weights) (Basheer

and Hajmeer, 2000; Maier and Dandy, 2000). Depending on the problem being solved, the success of training varies with selected factors.

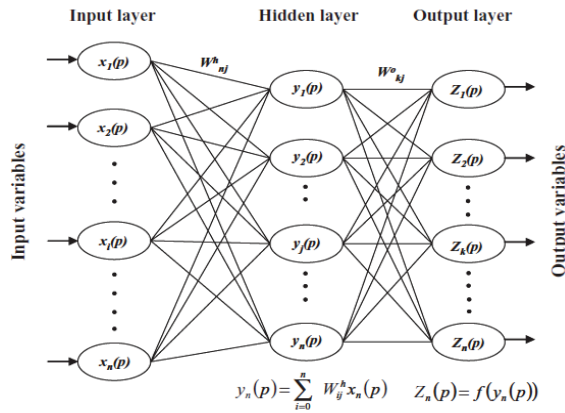


Fig. 2 A schematic structure of BPNN (one hidden layer)

Among all six variables, its correlative regression with ET_o was determined. Different combinations of input variables (number of combinations) were used in this study, 1, 2, 3, 4, 5 and 6 variables. The datasets of the following variables T_{min} , T_{avg} , T_{max} , RH, WS and RS, were used as the inputs and ET_o was used as the output. They were all daily averaged. Except for one individual variable used as an input, the rest of input combinations (two, three, four, five and six variables) were prepared to match solar radiation, which has the highest correlation regression with ET_o , with the others, which has the relatively high correlations (Table 1). A total of 20 combinations (from C_1 to C_{20}) were prepared to determine their best network

configuration and regression equation for BPNN and MLR. In further explanation, a combination 1 (C_1) to a combination 6 (C_6) has only one variable defined as input and a combination 7 (C_7) to a combination 11 (C_{11}) has two variables as inputs as per high correlation with ET_o .

To consider ANN modeling valid without manipulating data and/or evidence of contradictory results, all data used in this study was divided into three sets, one for the training, the other for the validation of the trained results, and another for the testing of the trained-validated results. A total of 1,633 datasets from 2010, 2012, 2014 to 2017 years were used, and 62% of data for network training, 8% for validation and 30% for testing were assigned, respectively. All meteorological input and output variables were standardized in the range of 0 to 1 using the Min-Max normalization method (Choi et al., 2018) and then partitioned using K-fold cross validation.

There is no established methodology for the selection of modeling parameters, such as the appropriate network architecture (the number of input, hidden and output layers), Processing Elements (PEs) in the hidden layer, the momentum, the learning rate, the learning rule and the transfer function in BPNN (Choi et al., 2018). Therefore, model convergence was based on the error function and exhibited any deviation between the predictions taken from corresponding target output values as the sum of the squares of the deviations. Training proceeded until the error was reduced to a desired minimum threshold. The most commonly used stopping criterion for neural network training was the sum-of-squared-error (SSE) which is presented in Equation (2) (Choi et al., 2018).

Table 1 Different combinations of input variables and its correspondent output variable

| No. of variables | Combination of Inputs | Output |
|------------------|--|--------|
| 1 | (C_1) T_{min} , (C_2) T_{avg} , (C_3) T_{max} , (C_4) RH, (C_5) WS, (C_6) SR | ET_o |
| 2 | (C_7) SR-RH, (C_8) SR- T_{avg} , (C_9) SR- T_{max} , (C_{10}) SR- T_{min} , (C_{11}) SR-WS | ET_o |
| 3 | (C_{12}) SR- T_{max} -RH, (C_{13}) SR- T_{max} - T_{avg} , (C_{14}) SR- T_{max} - T_{min} , (C_{15}) SR- T_{max} -WS | ET_o |
| 4 | (C_{16}) SR- T_{max} - T_{avg} -RH, (C_{17}) SR- T_{max} - T_{avg} - T_{min} , (C_{18}) SR- T_{max} - T_{avg} -WS | ET_o |
| 5 | (C_{19}) SR- T_{max} - T_{avg} - T_{min} -RH | ET_o |
| 6 | (C_{20}) SR- T_{max} - T_{avg} - T_{min} -RH-WS | ET_o |

Note: C stands for Combination

$$SSE = \sum_{i=1}^N (x_i - \bar{x}_i)^2 \quad (2)$$

where n is the number of output, x_i is the measured output and \bar{x}_i is the predicted output.

A PC-based neural network application software, NeuralWorks Professional II/Plus (Neuralworks®, Carnegie, Pennsylvania, USA) used in this study, allows users to adjust key network and training parameters in BPNN. Modifications are preferred to determine the best combination for solving the particular problem. Given the number of possible parameter combinations, the possibility of finding the correct combination of parameter settings, given a random starting point, is unlikely and is based primarily on chance (Kim et al., 2008).

MLR techniques can be used to model ET_o in terms of the local climatological parameters. The general purpose of the MLR model is to learn more about the relationship between several independent or predictor variables and a dependent or criterion variable. In MLR analysis, the values of ET_o were used as the dependent variable, while each combinations was used as independent variables to derive the coefficients in the MLR model. The regression equations were generated with the aid of Microsoft Excel in this study.

4. Performance evaluation criteria

The performance of BPNN and MLR models was evaluated by comparing their predictive accuracies with the ET_o values using Microsoft excel. The performance was characterized based on the following statistical criteria, which are R^2 (coefficient of determination), RMSE (root mean square error) and NSE (Nash-Sutcliffe efficiency) (Equation 3-5).

$$R^2 = \frac{\sum_{i=1}^N [A_i - \bar{T}]^2}{\sum_{i=1}^N [T_i - \bar{T}]^2} \quad (3)$$

$$RMSE = \sqrt{\frac{1}{N} \sum_{i=1}^N (A_i - T_i)^2} \quad (4)$$

$$NSE = 1 - \frac{\sum_{i=1}^N (A_i - T_i)^2}{\sum_{i=1}^N (A_i - \bar{A}_i)^2} \quad (5)$$

where, A_i and \bar{A}_i represent the FAO 56-PM estimate and its average for i th value; T_i and \bar{T}_i represent the BPNN (MLR)

computed values and their average for i th value; N represents the number of data considered.

III. RESULTS AND DISCUSSION

1. Meteorological condition of study area

The study area (Bushland, Texas, USA) has the meteorological condition which is categorized as semi-arid and has extremely variable precipitation temporally and spatially, which ranges from 400 to 560 mm. The area also has high evaporative demand, which is approximately 2,500 mm per year based on the Class A pan evaporation. This can be explained by high solar radiation, high vapor pressure deficit and strong regional advection. The monthly meteorological conditions in Bushland are plotted in Fig. 3.

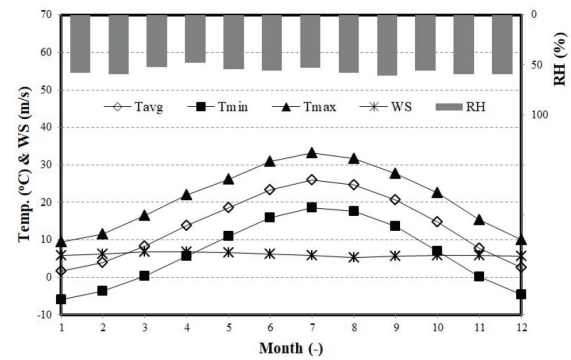


Fig. 3 Average meteorological conditions in Bushland

Table 2 presents the maximum, minimum, average and standard deviation (S.D.) values of temperature, relative humidity, wind speed, solar radiation and ET_o for the period of study. The multi-year average data for each meteorological variable were 17.13 °C (-14.57~30.85 °C) for Temp., 51.30% (7.40~99.92%) for RH, 5.16 m/s (0.31~9.67 m/s) for WS, 12.22 MJ/m²/day (0.81~27.38 MJ/m²/day) for SR and 4.66 mm/day (0.20~8.97 mm/day) for ET_o , respectively.

2. Relationship between meteorological variables and ET_o

Correlations of meteorological variables with ET_o are presented in Table 3. This table shows that the linear correlation between meteorological variables with ET_o ranged from 0.161 to 0.793. SR has the highest correlation with ET_o , which was

Table 2 Statistical parameters of daily meteorological variables in study area

| Year | | Temp. (°C) | RH (%) | WS (m/s) | SR (MJ/m ² /day) | ET _o (mm/day) |
|------|---------|---------------|-----------|-------------|--------------------------------|-----------------------------|
| 2010 | Max | 29,936 | 92,174 | 6,516 | 17,217 | 8,865 |
| | Min | 11,789 | 35,877 | 1,888 | 0,805 | 0,866 |
| | Average | 22,964 | 59,716 | 3,900 | 12,746 | 5,269 |
| | S.D. | 3,965 | 12,564 | 1,158 | 3,124 | 1,531 |
| 2012 | Max | 30,847 | 93,288 | 8,963 | 18,798 | 8,966 |
| | Min | -8,781 | 13,775 | 1,542 | 1,578 | 0,309 |
| | Average | 15,278 | 49,217 | 4,230 | 11,494 | 4,601 |
| | S.D. | 9,316 | 17,025 | 1,500 | 4,159 | 2,310 |
| 2014 | Max | 29,012 | 91,067 | 9,670 | 18,438 | 8,708 |
| | Min | -14,573 | 9,671 | 1,017 | 1,344 | 0,384 |
| | Average | 13,732 | 53,755 | 4,354 | 10,935 | 4,260 |
| | S.D. | 9,853 | 18,093 | 1,492 | 4,309 | 2,222 |
| 2015 | Max | 28,881 | 99,841 | 9,674 | 17,364 | 8,612 |
| | Min | -9,758 | 25,232 | 0,315 | 0,921 | 0,203 |
| | Average | 13,315 | 64,069 | 5,021 | 9,751 | 3,925 |
| | S.D. | 9,215 | 15,763 | 1,494 | 4,151 | 2,228 |
| 2016 | Max | 30,728 | 99,922 | 9,504 | 17,683 | 7,322 |
| | Min | -12,910 | 22,692 | 1,338 | 0,969 | 0,224 |
| | Average | 15,154 | 58,286 | 5,352 | 10,954 | 2,205 |
| | S.D. | 9,391 | 16,803 | 1,617 | 6,944 | 1,338 |
| 2017 | Max | 29,474 | 76,792 | 9,454 | 27,381 | 8,641 |
| | Min | 7,397 | 7,396 | 7,399 | 5,751 | 6,223 |
| | Average | 22,331 | 22,764 | 8,119 | 17,465 | 7,671 |
| | S.D. | 4,144 | 6,526 | 1,158 | 3,345 | 0,828 |

Table 3 Correlative regression between inputs and output for matching input combinations

| | T _{min} | T _{max} | T _{avg} | WS | RH | SR | ET _o |
|------------------|------------------|------------------|------------------|--------|--------|-------|-----------------|
| T _{min} | 1 | | | | | | |
| T _{max} | 0,859 | 1 | | | | | |
| T _{avg} | 0,949 | 0,965 | 1 | | | | |
| WS | -0,047 | -0,043 | -0,045 | 1 | | | |
| RH | 0,017 | -0,298 | -0,174 | -0,073 | 1 | | |
| SR | 0,592 | 0,754 | 0,724 | -0,032 | -0,417 | 1 | |
| ET _o | 0,626 | 0,783 | 0,751 | 0,161 | -0,540 | 0,793 | 1 |

followed by T_{max}, T_{avg}, T_{min}, RH and WS. This indicates that any BPNN and MLR models that use SR and T_{max} and/or T_{avg} as inputs may be able to estimate the ET_o to acceptable accuracy, depending on the specific application. The model's accuracy can be improved by implementing other variables that have aerodynamic effects of ET_o, such as RH and WS.

3. Performance comparison between BPNN and MLR models

There is no established methodology for the selection of the appropriate network architecture before training (Coulibaly et al., 2001; Jain et al., 2008; Wu et al., 2014). Therefore, this

study began with evaluating the number of hidden layer and PEs in the hidden layer which exhibit non-linear behavior between inputs and output. All other computational parameters (momentum, learning coefficient ratio, learning rule and transfer function) were also determined. The best performance per each combination was achieved and listed in Table 4. The trial and error procedure per each combination (C₁ through C₂₀) showed that just one hidden layer worked best and the number of PEs in the hidden layer ranged from 3 to 9. The best choice of momentum and learning rate are problem dependent and need some trial-and-error before good choices are found. In this study, the momentum that was used to modify the current

Table 4 Best architecture of BPNN and its computational parameters

| Combination | Input variables | No. of hidden layer | PEs of hidden layer | Momentum | Learning rate | Learning rule | Transfer function |
|-----------------|--|---------------------|---------------------|----------|---------------|---------------|-------------------|
| C ₃ | T _{max} | 1 | 3 | 0.4 | 0.5 | Norm-Cum-Del | Sine |
| C ₉ | SR-T _{max} | 1 | 4 | 0.4 | 0.5 | Delta | Tanh |
| C ₁₂ | SR-T _{max} -RH | 1 | 7 | 0.4 | 0.3 | Norm-Cum-Del | Tanh |
| C ₁₆ | SR-T _{max} -T _{avg} -RH | 1 | 4 | 0.4 | 0.5 | Delta | Tanh |
| C ₁₉ | SR-T _{max} -T _{avg} -T _{min} -RH | 1 | 9 | 0.4 | 0.5 | Ext DBD | Tanh |
| C ₂₀ | SR-T _{max} -T _{avg} -T _{min} -RH-WS | 1 | 9 | 0.4 | 0.5 | Delta | Tanh |

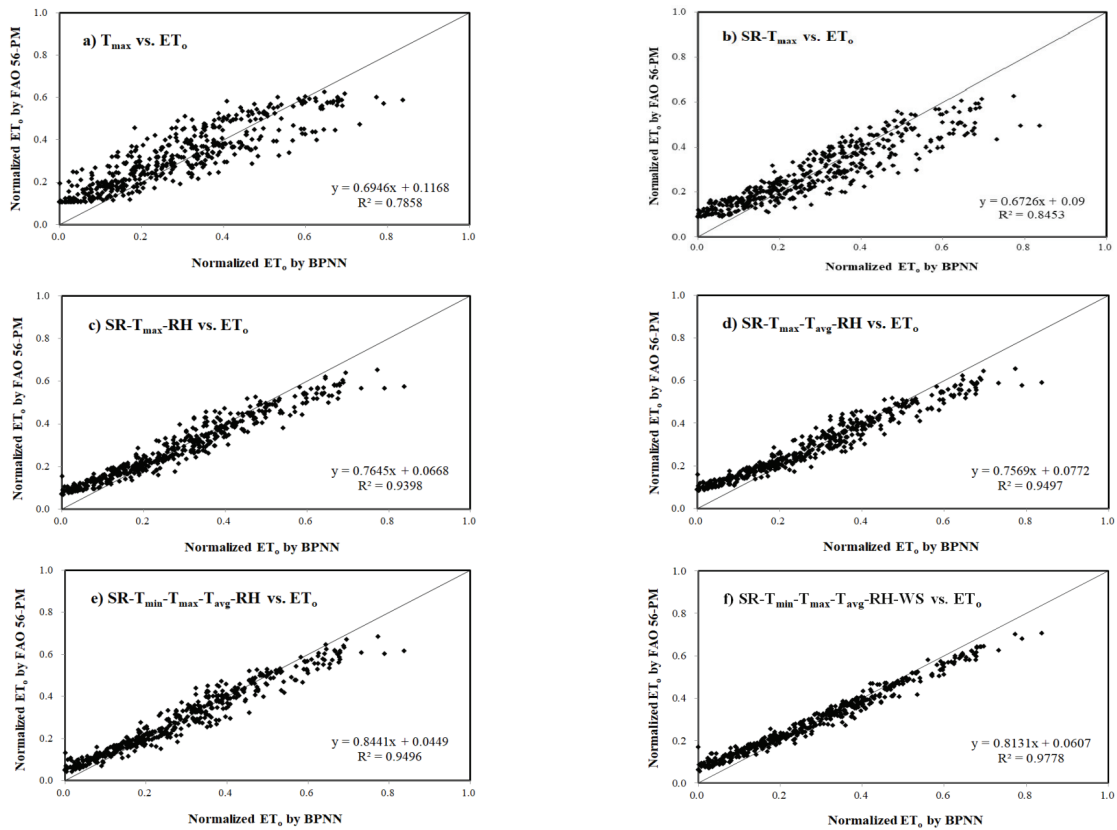


Fig. 4 Scattering diagrams of ET₀ estimated by BPNN and FAO 56-PM during the testing periods depending upon the combination of input

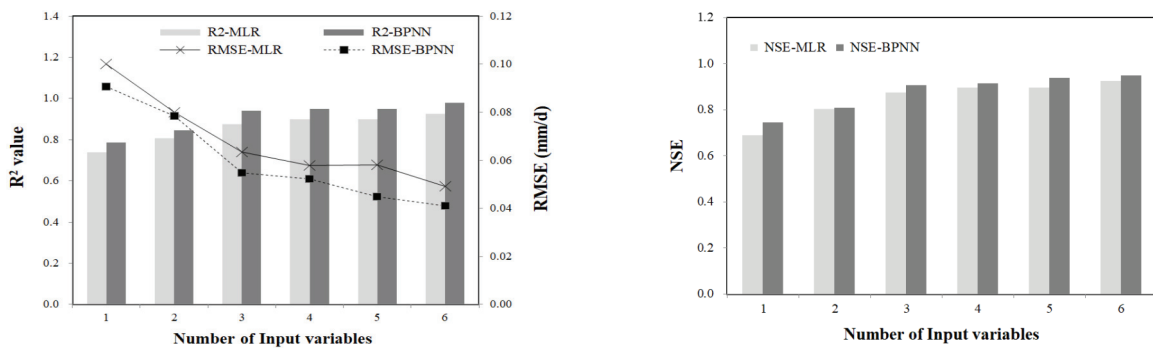
direction of computational movement in weight space based on previous changes was consistent as 0.4 for all combinations. Most combinations except for C₁₂ showed that the learning rate of 0.5 produced the best results, which indicates that no single value of learning rate was optimal for all combinations. The number of iterations was also considered one of the influencing factors on model performance and the preliminary test showed that more than 50,000 iterations did not improve the model accuracy (data not known). Instead of listing all twenty combinations, only the best performing combination per each group (same number of input variables used) is shown in Table

4, for example, C₃ was the best performing combination among C₁ through C₆.

Our analyses with ET₀ revealed that the performance criteria for the best BPNN model had the architecture of 6-1-1, which had one input layer of 6 neurons, one hidden layer of 1 neuron and one output layer of 1 neuron. The momentum and learning rate were initially set to 0.1 and 0.1, respectively. However, they were manipulated at 10 levels (increasing/decreasing by 0.1 from 0.0 to 1.0) in an effort to find the best configuration (0.4 of momentum and 0.3, 0.5 of learning rate). The optimal momentum and learning rate were finally determined to be

Table 5 Multiple Linear Regression equations per best combination

| Combination | Equation | R ² |
|-----------------|---|----------------|
| C ₃ | $Y = -0.168 + 0.805X_1$, where $X_1 = T_{\max}$ | 0.738 |
| C ₉ | $Y = -0.155 + 0.406X_1 + 0.443X_2$, where $X_1 = T_{\max}$, $X_2 = SR$ | 0.807 |
| C ₁₂ | $Y = 0.026 + 0.443X_1 - 0.272X_2 + 0.333X_3$, where $X_1 = T_{\max}$, $X_2 = RH$, $X_3 = SR$ | 0.876 |
| C ₁₆ | $Y = 0.093 - 0.073X_1 + 0.492X_2 - 0.342X_3 + 0.318X_4$, where $X_1 = T_{\max}$, $X_2 = T_{\text{avg}}$, $X_3 = RH$, $X_4 = SR$ | 0.899 |
| C ₁₉ | $Y = 0.061 + 0.107X_1 - 0.019X_2 + 0.364X_3 - 0.348X_4 + 0.323X_5$, where $X_1 = T_{\min}$, $X_2 = T_{\max}$, $X_3 = T_{\text{avg}}$, $X_4 = RH$, $X_5 = SR$ | 0.899 |
| C ₂₀ | $Y = -0.102 + 0.097X_1 + 0.031X_2 + 0.338X_3 + 0.349X_4 - 0.318X_5 + 0.323X_6$, where $X_1 = T_{\min}$, $X_2 = T_{\max}$, $X_3 = T_{\text{avg}}$, $X_4 = WS$, $X_5 = RH$, $X_6 = SR$ | 0.925 |


Fig. 5 Statistical comparison of model performance by BPNN and MLR

0.4 and 0.3(0.5) depending upon input combinations. In addition, the learning rules were varied, but the transfer function of hyperbolic tangent (Tanh) was superior to other functions.

The ability of BPNN modeling to predict daily ET_0 values using different combination of input variables was examined and their results are shown in Fig. 4. This figure only shows the case with the best modeling result per each BPNN modeling with different combination of input variables. Differently from the correlative regression results, the maximum air temperature had the greatest influence on ET_0 estimation when only one input variable was used for simulation. However, in the combinations with more than two input variables, SR showed the largest influence on model accuracy. The BPNN model underestimated and overestimated ET_0 at higher and smaller values, respectively, which may have resulted from diminished sensitivity of training to the more extreme ET_0 values. Even under this limitation, R^2 values ranged from 0.79 to 0.98.

In this study, the same training and validation datasets with BPNN modeling were used in generating the MLR equations and computing the coefficient of determination at a significance

level of 5% between the FAO 56-PM and MLR equations (Table 5). The smallest discrepancies between ET_0 calculated by BPNN and ET_0 calculated by the FAO 56-PM equation were achieved from C₃, C₉, C₁₂, C₁₆, C₁₉ and C₂₀ with 1, 2, 3, 4, 5 and 6 combination of input variables, respectively.

Fig. 5 shows the statistical comparison between BPNN and MLR models depending upon different combination of input variables. The values of R^2 , RMSE and NSE from BPNN modeling ranged from 0.786 to 0.978, from 0.005 to 0.091 (mm d^{-1}), and from 0.746 to 0.948, respectively. In combination of MLR modeling, values of R^2 , RMSE and NSE were from 0.738 to 0.925, from 0.049 to 0.100 (mm d^{-1}) and 0.691 to 0.925, respectively. This result showed that BPNN has a better performance than MLR, and both models indicate that no more than three input variables (T_{\max} , SR, RH) would improve the accuracy.

IV. CONCLUSIONS

Reference crop evapotranspiration (ET_0) plays a major role

in the agricultural management of water resources and its accurate prediction would signify better planning and management of the resources. Due to limitations of the FAO 56-PM equation, ANN modeling with BP algorithm was proposed as an alternative in this study to calculate ET_0 .

A total of twenty combinations with different combination of input variables were carefully selected and tested with ET_0 as an output. Both BPNN and MLR modeling provided the best results in ET_0 estimation using all meteorological variables as inputs, which was consistent with a study by Goel (2009) and Benzaghta et al. (2012) indicating that a combination of all input parameters provides better performance of the ANN model in estimating the ET_0 rather than individual parameters. However, this study found that even three most crucial inputs, T_{max} , RH and SR, when used in both BPNN and MLR models to accurately estimate ET_0 . This result was consistent with a study by Laaboudi et al. (2012). They were able to improve the temperature-based accuracy of a model using incomplete meteorological variables (air temperature, wind velocity and relative humidity) with the proper choice of ANN architecture. Also, they found that the temperature-based accuracy on ET_0 estimation was improved by incorporating with wind velocity and relative humidity as the network input datasets.

A study by Landeras et al. (2008) compared between ANNs and alternative evapotranspiration equations with lower input requirements to the FAO 56-PM equation. They found that ANNs based on the same inputs, as those required for the application of the FAO 56-PM equations with or without solar radiation or relative humidity, gave a better performance than their analogous linear calibrated equations (the FAO 56-PM based equation with estimated solar radiation and/or relative humidity).

However, it should be noted that the correlation between ET_0 and meteorological variables could be different over regions, which means that the highest and lowest correlations with ET_0 were SR and WS in this study, but it could be different in other area. This indicates that it should include more data to train, validate and test BPNN to function as a universal model.

Overall, this study showed that the possibility of estimating ET_0 with lesser number of meteorological variables as inputs and could provide valuable information on irrigation scheduling in an easily accessible way.

ACKNOWLEDGEMENT

This study was carried out with the support of the Research Program for Agricultural Science & Technology Development (Project No. PJ012748012019), National Institute of Agricultural Sciences (NAS), Rural Development Administration, Republic of Korea.

REFERENCES

1. Abedi-Koupai, J., M. J. Amiri, and S. Eslamian, 2009. Comparison of artificial neural network and physically-based models for estimating of reference evapotranspiration in greenhouse. *Australian Journal of Basic and Applied Sciences* 3(3): 2528-2535.
2. Allen, R. G., L. S. Pereira, D. Raes, and M. Smith, 1998. Crop evapotranspiration-Guidelines for computing crop water requirements. FAO Irrigation and Drainage Paper, No 56, FAO, Rome.
3. Allen, R. G., W. O. Pruitt, J. L. Wright, T. A. Howell, F. Ventura, R. Snyder, D. Itenfisu, P. Steduto, J. Berengena, J. B. Yrisarry, M. Smith, L. S. Pereira, D. Raes, A. Perrier, A. Alves, I. Walter, and R. Elliot, 2006. A recommendation on standardized surface resistance for hourly calculation of reference ET_0 by the FAO 56 Penman-Monteith method. *Agricultural Water Management* 81(1-2): 1-22.
4. Allen, R. G., L. S. Pereira, T. A. Howell, and M. E. Jensen, 2011. Evapotranspiration information reporting: II. Recommended documentation. *Agricultural Water Management* 98: 921-929
5. Basheer I. A., and M. Hajmeer, 2000. Artificial neural networks: Fundamentals, computing, design, and application. *J. Microbiol. Methods* 43(1): 3-31.
6. Benzaghta, M. A., T. A. Mohammed, and A. I. Ekhmaj, 2012. Prediction of evaporation from Algardabiya reservoir. *Libyan Agriculture Research Center Journal International* 3: 120-128. doi:10.5829/idosi.larcji.2012.3.3.1205.
7. Choi, Y., M. Kim, S. O'Shaughnessy, J. Jeon, Y. Kim, and W. Song, 2018. Comparison of artificial neural network and empirical models to determine daily reference evapotranspiration. *Journal of the Korean Society of Agricultural Engineers* 60(6): 43-54. doi:10.5389/KSAE.2018.60.6.043.
8. Coulibaly, P., F. Anctil, R. Aravena, B. Bobée, 2001.

- Artificial neural network modeling of water table depth fluctuations. *Water Resources Research* 37(4): 885-896. doi:10.1029/2000WR900368.
9. Dai, X., H. Shi, Y. Li, Z. Ouyang, and Z. Huo, 2009. Artificial neural network models for estimating regional reference evapotranspiration based on climate factors. *Hydrological Processes* 23: 442-450. doi:10.1002/hyp.7153.
 10. Djman, K., K. Lombard, K. Komlan, and S. Allen, 2018. Variability of the ratio of alfalfa to grass reference evapotranspiration under semiarid climate. *Irrigation & Drainage Systems Engineering* 7(204): 1-6. doi:10.4172/2168-9768.1000204.
 11. Drexler, J. Z., R. L. Snyder, D. Spano, and U. K. T. Paw, 2004. A review of models and micrometeorological methods used to estimate wetland evapotranspiration. *Hydrological Processes* 18(11): 2071-2101. doi:10.1002/hyp.1462.
 12. George, B. A., B. R. S. Reddy, N. Raghuvanshi, and W. W. Wallender, 2002. Decision support system for estimating reference evapotranspiration. *Journal of Irrigation and Drainage Engineering* 128(1): 1-10. doi:10.1061/ASCE.0733-9437.
 13. Goel, A., 2009. ANN based modeling for prediction of evaporation in reservoirs (Research Note). *International Journal of Engineering, Transactions A: Basics* 22(4): 351-358.
 14. Haykin, S., 1998. *Neural networks: A comprehensive foundation*. Prentice-Hall, Englewood Cliffs.
 15. Itenfsu, D., R. L. Elliott, R. G. Allen, and I. A. Walter, 2003. Comparison of reference evapotranspiration calculations as part of the ASCE standardization effort. *Journal of Irrigation and Drainage Engineering* 129(6): 440-448. doi:10.1061/ASCE.0733-9437.
 16. Jain S. K., A Sarkar, and V. Garg, 2008. Impact of declining trend of flow on Harike Wetland, India. *Water Resources Management* 22(4): 409-421. doi:10.1007/s11269-007-9169-9.
 17. Jennifer, M. J., and R. S. Sudheer, 2001. Evaluation of reference evapotranspiration methodologies and AFSIRS crop water use simulation model. Final report, Division of Water Supply Management, St. Johns River Water Manag. Dist., Palatka, Florida.
 18. Jensen, M. E., R. D. Burman, and R. G. Allen, 1990. *Crop and irrigation water requirements. Manual and Reports on Engineering Practice No. 70*, ASCE, New York.
 19. Kecman, V., 2001. *Learning and soft computing*. London, England: MIT press.
 20. Khoob, A. R., 2008. Comparative study of Hargreaves's and artificial neural network's methodologies in estimating reference evapotranspiration in a semiarid environment. *Irrigation Sci.* 26(3): 253-259. doi:10.1007/s00271-007-0090-z.
 21. Kim, M., C. Y. Choi, and C. P. Gerba, 2008. Source tracking of microbial intrusion in water system using artificial neural networks. *Water Research* 42(4-5): 1308-1314. doi:10.1016/j.watres.2007.09.032.
 22. Laaboudi A., B. Mouhouche, and B. Draoui, 2012. Conceptual reference evapotranspiration models for different time steps. *Journal of Petroleum & Environmental Biotechnology* 3(4): 1-8. doi:10.4172/2157-7463.1000123.
 23. Landeras G., A. Ortiz-Barredo, and J. J. López, 2008. Comparison of artificial neural network models and empirical and semi-empirical equations for daily reference evapotranspiration estimation in the Basque Country (Northern Spain). *Agricultural Water Management* 95: 553-565. doi:10.1016/k/agwat/2007.12.011.
 24. Lee, E. J., M. S. Kang, J. A. Park, J. Y. Choi, and S. W. Park, 2010. Estimation of future reference crop evapotranspiration using artificial neural networks. *Journal of the Korean Society of Agricultural Engineers* 52(5): 1-9. doi:10.5389/KSAE.2010.52.5.001.
 25. Lu, Y., D. Ma, X. Chen, and J. Zhang, 2018. A simple method for estimating field crop evapotranspiration from Pot Experiments. *Water* 10: 1-19. doi:10.3390/210121823.
 26. Maier, H. R., and G. C. Dandy, 2000. Neural networks for the prediction and forecasting of water resources variables: A review of modeling issues and applications. *Environmental Model. Software* 15: 101-124. doi:10.1016/S1364-8152(99)00007-9.
 27. Mia, M. M., S. K. Biswas, and M. C. Urmi, 2015. An algorithm for training multilayer perceptron (MLP) For image reconstruction using neural network without overfitting. *IJSTR* 10: 271-275.
 28. Palayasoot, P., 1965. Estimation of pan evaporation and potential evapotranspiration of rice in the central plain of Thailand by using various formulas based on climatological data. M. S. Thesis, College of Engineering, Utah State University, Logan.
 29. Parisi, S., L. Mariani, G. Cola, and T. Maggiore, 2009. Mini-lysimeters evapotranspiration measurements on

- suburban environment. *Italian Journal of Agrometeorology* 3: 13-16.
30. Smith, M., R. G., Allen, J. L. Monteith, A. Perrier, L. Pereira, and A. Seegeren, 1992. Report of the expert consultation on procedures for revision of FAO guidelines for prediction of crop water requirements. UN-FAO, Rome, Italy, 54p.
31. Sudheer, K. P., and S. K. Jain, 2003. Radial basis function neural networks for modeling stage discharge relationship. *J. Hydrol. Eng.* 8(3): 161-164.
32. Traoré, A., H. H. Tamboura, A. Kaboré, L.J. Royo, I. Fernández, I. Álvarez, M. Sangaré, D. Bouchel, J. P. Poivey, L. Sawadogo, and F. Goyache, 2008. Multivariate analyses on morphological traits in Burkina Faso goat. *Arch Anim Breed* 51: 588-600. doi:10.1016/j.smallrumres.2008.09.011.
33. Vyas, K. N., and R. Subbaiah, 2016. Application of artificial neural network approach for estimating reference evapotranspiration. *Current World Environment* 11(2): 637-647. doi:10.12944/CWE.11.2.36.
34. Zanetti, S. S., E. F. Sousa, V. P. S. Oliveira, F. T. Almeida, and S. Bernardo, 2007. Estimating evapotranspiration using artificial neural network and minimum climatological data. *Journal of Irrigation and Drainage Engineering* 133(2): 83-89. doi:10.1061/(ASCE)0733-9437(2002)128:4(224).
35. Wu, W., G. C. Dandy, and H. R. Maier, 2014. Protocol for developing ANN models and its application to the assessment of the quality of the ANN model development process in drinking water quality modeling. *Environ. Model. Softw.* 54: 108-127. doi:10.1016/j.envsoft.2013.12.016.